Zhang *et al. Molecular Cancer* (2024) 23:198
https://doi.org/10.1186/s12943-024-02116-6

Molecular Cancer

RESEARCH Open Access

Exosomal miR-4745-5p/3911 from N2-polarized tumor-associated neutrophils promotes gastric cancer metastasis by regulating SLIT2

Jiahui Zhang[1,3], Dan Yu[1], Cheng Ji[1], Maoye Wang[1], Min Fu[1], Yu Qian[1], Xiaoxin Zhang[1], Runbi Ji[1], Chong Li[3*], Jianmei Gu[2*] and Xu Zhang[1*]

Abstract

Tumor cells remodel the phenotype and function of tumor microenvironment (TME) cells to favor tumor progression. Previous studies have shown that neutrophils in TME are polarized to N2 tumor-associated neutrophils (TANs) by tumor derived factors, thus promoting tumor growth and metastasis, angiogenesis, therapy resistance, and immunosuppression. Exosomes act as critical intercellular messengers in human health and diseases including cancer. So far, the biological roles of exosomes from N2 TANs in gastric cancer have not been well characterized. Herein, we represented the first report that exosomes from N2 TANs promoted gastric cancer metastasis in vitro and in vivo. We found that exosomes from N2 TANs transferred miR-4745-5p/3911 to gastric cancer cells to downregulate SLIT2 (slit guidance ligand 2) gene expression. Adenovirus-mediated overexpression of SLIT2 reversed the promotion of gastric cancer metastasis by N2 TANs derived exosomes. We further revealed that gastric cancer cells induced glucose metabolic reprogramming in neutrophils through exosomal HMGB1 (high mobility group protein B1)/NF-κB pathway, which mediated neutrophil N2 polarization and miR-4745-5p/3911 upregulation. We further employed ddPCR (droplet digital PCR) to detect the expression of miR-4745-5p/3911 in N2 TANs exosomes from human serum samples and found their increased levels in gastric cancer patients compared to healthy controls and benign gastric disease patients. Conclusively, our results indicate that N2 TANs facilitate cancer metastasis via regulation of SLIT2 in gastric cancer cells by exosomal miR-4745-5p/3911, which provides a new insight into the roles of TME cells derived exosomes in gastric cancer metastasis and offers a potential biomarker for gastric cancer diagnosis.

Keywords Exosomes, Gastric cancer, Tumor-associated neutrophils, N2 polarization, Metastasis, SLIT2

*Correspondence:
Chong Li
lichong1705@163.com
Jianmei Gu
gujianmei2010@163.com
Xu Zhang
xuzhang@ujs.edu.cn

[1]Department of Laboratory Medicine, School of Medicine, Jiangsu University, Zhenjiang, Jiangsu 212013, China
[2]Departmemt of Clinical Laboratory Medicine, Nantong Tumor Hospital/Affiliated Tumor Hospital of Nantong University, Nantong, Jiangsu 226300, China
[3]Kunshan Biomedical Big Data Innovation Application Laboratory, Affiliated Kunshan Hospital of Jiangsu University, Kunshan, Jiangsu 215300, China

Introduction

Gastric cancer (GC) is one of the leading causes of cancer-related death worldwide. Tumor microenvironment (TME) plays an important role in the pathogenesis of gastric cancer. TME is a complex and dynamic ecosystem consisting of tumor cells and distinct non-tumor cells, such as stromal cells, immune cells, and endothelial cells. Further understanding of cellular interactions within TME would contribute to the discovery of new biomarkers and therapeutic targets. Tumor-associated neutrophils (TANs) play dual roles in tumors and the N1/N2 paradox has been proposed, in which N1 TANs possess anti-tumor while N2 TANs exert pro-tumor activities [1, 2]. Previous studies by others and our group have identified the diverse roles of N2 TANs in cancer progression and a close relationship between tumor-infiltrating neutrophils and poor prognosis in cancer patients [3–5].

Exosomes act as important messengers between tumor cells and TME cells [6]. Early studies suggest that tumor cell-derived exosomes modulate the phenotype and function of TME cells, which in turn promotes tumor growth, metastasis, and therapy resistance. Recent studies indicate that TME cell-derived exosomes also contain various bioactive molecules and participate in the regulation of tumor malignancy. For instance, exosomes from M2 tumor-associated macrophages (TAMs) and cancer-associated fibroblasts (CAFs) have been reported to play versatile roles in tumor development and progression [7, 8]. However, the biological role of TAN-derived exosomes in cancer has not been well characterized.

An increasing number of studies suggest a key role of neutrophil-derived exosomes in the pathogenesis of inflammatory diseases [9–11]. In human chronic obstructive pulmonary disease (COPD), activated neutrophils release pathogenic exosomes containing surface-bound and αl-antitrypsin (α1AT)-resistant neutrophil elastase (NE) [12]. These exosomes bind and degrade the extracellular matrix (ECM) via integrin Mac-1 and NE, bypassing the pulmonary antiprotease barrier to induce ECM destruction. Moreover, neutrophil-derived exosomes can be detected in clinical specimens from COPD patients and are capable of transferring a COPD-like phenotype from humans to mice in an NE-dependent manner. Using a high-fat diet-induced atherosclerosis mouse model, Gomez et al. demonstrate that neutrophil microvesicles accumulate in disease-prone regions of arteries to promote vascular inflammation [13]. Neutrophil microvesicles deliver miR-155 to activate NF-κB and promote inflammatory gene expression in endothelial cells exposed to disturbed flow, which results in increased recruitment of monocytes to the vessel wall and enhanced atherosclerotic plaque formation. In a lipopolysaccharide (LPS)-challenged sepsis mouse model, circulating neutrophils migrate along the vascular endothelium and release mitochondrion-containing exosomes that transport substantial Sod2 (superoxide dismutase 2) to clear intravascular ROS and maintain endothelium homeostasis, mitigating the occurrence of disseminated intravascular coagulation (DIC) [14]. These findings strongly imply that neutrophil exosomes deliver bioactive cargos to play multifaceted roles in disease progression, which may have been previously overlooked as a result of the short lifespan of neutrophils.

Recently, neutrophil-derived exosomes have been reported to be involved in tumor development and progression by delivering mRNA, miRNAs, and piRNAs [15]. For instance, neutrophil-derived exosomes deliver SPI1 (salmonella pathogenicity island 1) mRNA to colorectal cancer cells to drive glycolysis and tumor progression [16]. Tyagi et al. demonstrate that N2 neutrophils secrete exosomal miR-4466 to promote the stemness and glycolysis of lung cancer cells, thereby enhancing brain metastasis [17]. Moreover, senescent neutrophils promote chemoresistance in breast cancer via exosomal piRNA-17,560 [18]. These findings establish a critical role for neutrophil-derived exosomes in cancer. Previously, we demonstrated that gastric cancer cell-derived exosomes induce neutrophil N2 polarization, which in turn promotes the metastatic ability of gastric cancer cells [4]. Herein, we hypothesized that N2-polarized neutrophils secrete exosomes to deliver miRNAs into gastric cancer cells, forming a positive cellular crosstalk in the TME to drive gastric cancer metastasis.

Materials & methods

Ethics statement for human samples and animal models

Serum samples from patients with gastric cancer (GC, $n=85$) or benign gastric diseases (BGD, $n=60$) and healthy controls (HC, $n=85$) were obtained from the Affiliated People's Hospital of Jiangsu University. All clinical samples enrolled in this study were identified and diagnosed between March 2021 and August 2023 at the Affiliated People's Hospital of Jiangsu University. The clinical characteristics of patients are listed in Table S1. Written informed consent was obtained from all participants. The study was carried out in accordance with the clinical study protocol by institutional review board at the Affiliated People's Hospital of Jiangsu University and conducted in accordance with the ethical principles of the World Medical Association Declaration of Helsinki. The animal experimental protocols were approved by the Animal Care and Use Committee of Jiangsu University (Approval number: 2020280). All animal experiments were performed in accordance with the associated relevant guidelines and regulations for working with live vertebrate animals.

Neutrophil isolation and treatment

Peripheral blood samples were collected from healthy volunteers after obtaining written informed consent. The study was approved by the Ethics Committee of Jiangsu University. Neutrophils were isolated from the peripheral blood by using polymorphprep (Axis-Shield, Norway). RBCs were lysed using hypotonic lysing procedure. The purified neutrophils (N1-neutrophils) were seeded in RPMI 1640 with 10% fetal bovine serum (FBS, exosome-depleted) and the culture medium was collected for 24 h.

Neutrophils isolated from peripheral blood were treated with exosomes from gastric cancer cells (GC-Exo; 30 μg/mL) for 12 h to differentiate into N2-polarized neutrophils. Then, GC-Exo induced, N2-polarized neutrophils were cultured in RPMI 1640 supplemented with 10% of exosome-free FBS for 24 h and the conditioned medium (CM) was collected.

Peripheral blood samples were obtained from gastric cancer patients and low density neutrophils (LDNs) and high density neutrophils (HDNs) were isolated by using double-gradient percoll separation assay. Briefly, peripheral blood drawn in the heparin tubes was mixed with 3% dextran and incubated for 30 min. The blood samples were centrifuged at 200 × g for 25 min and 400 × g for 15 min. The LDNs under the plasma layer and the HDNs at the bottom of percoll layers were collected and cultured in RPMI 1640 medium for further study.

Exosome isolation and characterization

Neutrophils derived CM were collected and centrifuged at 800 × g for 10 min, 2000 × g for 10 min, and 10 000 × g for 30 min and then filtered by using 100 KDa ultrafiltration centrifugal tube. The supernatant was centrifuged at 100,000 × g for 80 min. The supernatant (defined as CM depleted of Exo) was removed and the pellet was resuspended in phosphate buffer (PBS). Protein concentration was determined using a BCA protein assay kit (ThermoFisher, USA). The size and concentration of the exosomes were analyzed using nanoparticle tracking analysis (Particle Metrix, Germany). The morphology of the purified exosomes was examined by transmission electron microscopy (Philips, Netherlands) and atomic force microscopy (Veeco, USA), and the polydispersity index of the exosomes was measured by dynamic light scattering. The exosomal markers CD9, CD63, CD81, and Alix (Cell signaling technology, USA), and the ER marker calnexin (Abcam, UK) were detected by western blotting.

Exosome internalization assays

HGC27 cells (3×10^5/well) were seeded in 12-well plates and incubated for 12 h. Exosomes were labeled with the membrane fluorescent dye DiR (5 μM) and added to HGC27 cells for uptake studies. After incubation for 3, 6, or 9 h at 37 °C, cells were fixed with 4% paraformaldehyde and permeabilized in 0.2% Triton X-100. Cell nucleis were stained with DAPI for 10 min followed by detection using multidimensional panoramic flow cytometry and fluorescence confocal laser microscopy. To identify the transfer of exosomes derived miRNAs, Cy3-labeled miR-4745-5p and miR-3911 were transfected into neutrophils. Cy3-miR-4745-5p and miR-3911 expressing neutrophils were co-cultured with HGC27 cells. The internalization of miR-4745-5p and miR-3911 by HGC27 cells was measured using confocal microscopy.

Cell culture and treatment

Human gastric cancer cell line (HGC27) and human umbilical vein endothelial cell line (HUVEC) were purchased from Procell Life Science & Technology (Wuhan, China). Human gastric cancer cell line (MGC803) and cancer-associated fibroblasts (CAF) were purchased from Fenghui Biotechnology (Shanghai, China). These cells were cultured in RPMI 1640 medium containing 10% FBS at 37 °C. In some experiments, GW4869 (Sigma, USA) was used as an inhibitor for exosomes release. GW4869 (20 μM) was added into the culture system for 12 h. Neutrophils were pretreated with NF-κB pathway inhibitor Bay11-7082 (10 μM) and collected for gene and protein detection.

Western blot analysis

Cells or exosomes were lysed in RIPA buffer containing proteinase inhibitors (Sigma, USA). A total of 20 μg of protein per sample was loaded onto a 12% SDS-PAGE gel and transferred to a polyvinylidene difluoride (PVDF) membrane. Membranes were blocked with 5% non-fat milk and incubated overnight with primary antibodies. Antibodies against PFKFB3, LDHA, HK-2, PKM2, G6PD, N-cadherin, E-cadherin, Vimentin, Oct4, Sox2, Nanog, ZEB2, SNAIL, Twist, ALDH1A1, SLIT2, p-p65, p65, p-p38, p38, p-Akt, Akt, p-ERK, ERK, CD9, CD63, CD81, Alix, and Calnexin were purchased from Cell Signaling Technology (Danvers, USA). The membranes were then incubated with HRP-conjugated goat anti-rabbit or anti-mouse secondary antibodies (Bioworld, USA) after washing three times with TBST. The membranes were visualized with a thermo pierce chemiluminescent (ECL) western blotting substrate (ThermoFisher, USA) using a Tanon 5200 system. β-actin served as the loading control.

RNA sequencing and bioinformatics analysis

Total RNAs were extracted from the exosomes using the total exosome RNA and protein isolation kit (Invitrogen, USA). The amount and quality of small RNA in the total RNA were detected using Ribo kit (Guangzhou, China). Small RNA library construction and sequencing were performed by OE Biotech (Shanghai, China). The cDNA library was sequenced on an Illumina HiSeq 2500.

Raw reads were collected using Illumina analysis software. Briefly, the RNA sequencing data were compared with the reference genome or transcriptome. The fragments per kilobase of exon model per million mapped fragments (FPKM) and transcript per million (TPM) were used to quantify the expression levels of genes or transcripts. Then, we compared gene expression differences in each sample, and presented the bioinformatics data in the form of images and tables. We utilized the online miRNA target prediction software such as miRDB (http://www.mirdb.org/) to identify the common target genes of miR-4745-5p and miR-3911 and listed in Table S2.

Luciferase reporter assay

Fragments of the SLIT2 3′-untranslated region (3′-UTR) containing either putative miR-4745-5p or miR-3911 seed sequences were synthesized by GeneChem (Shanghai, China). Cells cultured in 24-well plates were transfected with control vector, wild-type or mutant SLIT2 3′-UTR psiCHECK-2 plasmid (Promega, USA), miR-4745-5p/3911 mimics or miR-4745-5p/3911 inhibitor (RiboBio, China) by using lipofectamine 3000 (Invitrogen, USA). After transfection for 48 h, the luciferase activities were measured using the dual-luciferase report assay kit. Renilla luciferase activity was used for normalization. The fold change of each miRNA compared to NC was calculated.

Quantitative real-time PCR

Total RNA from treated cells was extracted using trizol reagent (Invitrogen, USA), and complementary DNA was synthesized using the reverse transcription system (Vazyme, China) according to the manufacturer's instructions. Relative gene expression was normalized to that of U6 and β-actin using the $2^{-\Delta\Delta Ct}$ comparative method. Primers for miR-4745-5p, miR-3911, and U6 were purchased from RiboBio, and their sequences are listed in Table S3. The primers of genes related to epithelial-mesenchymal transition (EMT), cell stemness and glucose metabolism were synthesized by Sangon Biotech (Shanghai, China). Real-time quantitative PCR was performed using SYBR green PCR master mix (Cwbio, China) on a Bio-Rad CFX96 detection system. All samples were tested thrice.

Cell migration and invasion assays

The effect of exosomes (50 μg/mL) on the migration and invasion of gastric cancer cells was detected using transwell 24-well plates (8-μm pores; Corning, USA). For migration assays, cancer cells (5×10^4/well) suspended in 200 μL of serum-free medium were seeded into the top chamber, and complete medium (600 μL) was added to the lower chamber. After incubation for 12 h, the migrated cells were fixed with paraformaldehyde, stained with crystal violet, and observed under a microscope (CKX41; Olympus, Japan). For invasion assays, the insert membranes were coated with matrigel (50 μL/well; BD Biosciences) before adding the cells. After culturing for 24 h, cells were fixed, stained with 0.1% crystal violet for 30 min, and counted under a microscope.

Colony formation assay

Briefly, the gastric cancer cells were cultured in six-well plates (1×10^3/well) and incubated for 12 days after receiving different treatments (N2-Exo; 50 μg/mL). At the end of the experiment, colonies were fixed with 4% paraformaldehyde and stained with crystal violet. Visible colonies containing more than 50 cells were counted.

Cell transfection

The miR-4745-5p and miR-3911 mimics and inhibitors (2'-O-methyl modification) were synthesized by RiboBio. Gastric cancer cells (2×10^5/well) were seeded in 6-well plates and cultured overnight at 37 °C. When cells reached 50% confluence, miRNA mimics (50 nM) or miRNA inhibitors (100 nM) were transfected with lipofectamine 3000 according to the manufacturer's instructions (Life technologies, USA). Six hours after transfection, the cells were changed to complete medium for another 24 h and harvested for subsequent experiments.

Spheroid formation assay

For spheroid formation assay, gastric cancer cells (5×10^3/well) were plated in 6-cm low-adherence cell culture dishes and cultured in serum-free RPMI-1640 medium (Gibco, USA) containing 20 ng/mL epidermal growth factor (EGF; ThermoFisher, USA), 10 ng/mL basic fibroblast growth factor (bFGF; ThermoFisher, USA) and 10 μg/mL B27 supplement (Gibco, USA). Two weeks later, the number of spheroids (diameter>75 μm) per well was counted under a light microscope (IX70, Olympus, Japan) and quantified using ImageJ software. The experiments were repeated at least thrice.

RNA interference

The HMGB1 siRNA sequence was CCGUUAUGAAAG AGAAAUGAAU, and the scramble control was UUCUC CGAACGUGUCACGUAA. Cells were collected for further studies 24, 48, and 72 h after transfection. HMGB1 siRNA (Genepharma, China) at a final concentration of 100 nM was transfected into cancer cells using lipofectamine 3000.

Droplet digital PCR and data analysis

All ddPCR experiments were performed and analyzed following the same workflow as previously reported [19,

20]. Briefly, each PCR was performed in a final volume of 25 μL, containing 5 μL of 5 × PerfeCTa Multiplex qPCR ToughMix (Quanta BioSciences, USA), 2.5 μL of 1 μM Fluorescein (VWR, USA), 2.5 μL of homemade 10 × ESR1 assay and 15 μL of input cfDNA sample. The samples were then diluted in DNase/RNase-free ultra-pure distilled water (Invitrogen, USA) to achieve a maximum theoretical concentration of 10,000 copies/PCR and performed a PCR amplification cycle. The chips were imaged with the Naica Prism3 scanner using crystal reader software v2.4.0.3, with optimized parameters, and analyzed using crystal miner software v2.4.0.3.

Analysis of glucose metabolism in neutrophils

The effect of GC-Exo on the expression of glycolytic genes and proteins in neutrophils was analyzed by qRT-PCR and western blot assays. After treatment with GC-Exo, neutrophils were collected for the measurement of lactate concentration and glucose consumption. Glucose uptake and lactate production were detected by using glucose uptake assay kit and lactate assay kit (Sigma, USA). The ATP level and cellular LDH activity of neutrophils were measured by ATP assay kit and lactate dehydrogenase assay kit (Beyotime, China).

Glucose-6-phosphate dehydrogenase activity assay kit (G6PDH-1-Y, Comin Biotechnology, China) and NADPH oxidase activity assay kit (NOX-1-Y, Comin Biotechnology, China) were used to detect the enzyme activity of neutrophils treated with GC-Exo. Neutrophils isolated from peripheral blood were added to 12-well plates (1×10^6/well) and incubated with GC-Exo in the presence or absence of diphenyleneiodonium chloride (DPI) for 12 h. Then, the cells were collected and resuspended in lysis buffer for sonicating. The G6PD and NOX enzyme activities of cell lysate supernatant were measured at 403/600 nm by using microplate reader.

Animal experiments

Six-week-old female BALB/c nude mice were purchased from the model animal research center at nanjing university. All animal studies were conducted according to protocols approved by the Ethics Committee of Jiangsu University. HGC27-luciferase cells were intraperitoneally injected into mice to construct peritoneal metastasis models (5×10^6 cells per mouse; $n=5$/group) and intravenously injected into mice to construct a lung metastasis model (3×10^5 cells per mouse; $n=5$/group). CM or exosomes (10 mg/kg body weight; 100 μL) were then injected into the caudal veins every 4 days. Metastatic lesions were detected by bioluminescence imaging using an IVIS Lumina II (PerkinElmer, USA). Animals were sacrificed 6 weeks after treatment, and lung metastases were examined using H&E staining. For tumor growth study, HGC27 (3×10^6 cells per mouse; $n=5$/group) were subcutaneously injected into the flanks of BALB/c nude mice. When the tumor sizes grew to 60 mm^3, exosomes (10 mg/kg body weight; 100 μL) were intratumorally injected into the mice. The tumor size and survival periods of each group were monitored.

Statistical analysis

All in vitro experiments were performed at least in triplicate for each group and statistical analyses were performed using GraphPad Prism 7.0 (GraphPad Software, San Diego, CA, USA). Data are represented as the mean ± SD. One-way analysis of variance (ANOVA) for multiple groups and Student's t-test for two groups were used for statistical analysis. Survival time was analyzed using the Kaplan-Meier method and log-rank test. Receiver operating characteristic (ROC) curves and the area under ROC curve (AUC) were established to determine the sensitivity and specificity of miRNAs for early tumor diagnosis. Spearman's correlation analysis was conducted to evaluate whether the expression levels of miRNAs were correlated with common target SLIT2. A value of $P<0.05$ was considered statistically significant.

For The Cancer Genome Atlas (TCGA) database analysis, the intersection of each top 20% high-expression samples was defined as synergistic high, and the intersection of each bottom 20% low expression samples was served as synergistic low to evaluate the combinational effect of miR-4745-5p and miR-3911.

Results

N2-polarized neutrophils promote the metastatic potential of gastric cancer cells through exosomes

Recent studies have suggested that exosomes from the tumor microenvironment (TME) cells play an important role in tumor development and progression [6–8]. To understand the role of exosomes from N2-polarized neutrophils (N2-Exo) in gastric cancer, we collected exosomes from N2-polarized neutrophils and identified them by TEM, AFM, NTA, Zeta-view (Fig. 1A and D) and western blotting (Figure S1A). Next, we used N2-Exo to treat gastric cancer cells and used N2-CM and N2-CM depleted of exosomes as controls. The internalization of N2-Exo by gastric cancer cells was verified by imaging flow cytometry and immunofluorescence staining (Figures S1B and S1C). Exosomes from different samples exhibited similar morphological characteristics, size and particle numbers, suggesting that our exosome extraction methods are stable and reliable for the following experiments (Figure S2). The results of transwell migration and matrigel invasion assays showed that, similar to N2-CM, N2-Exo treatment greatly improved the metastatic ability of gastric cancer cells in vitro (Fig. 1E and G), whereas N2-CM depleted of Exo had minimal effects. The results of the cell scratch assay also showed similar

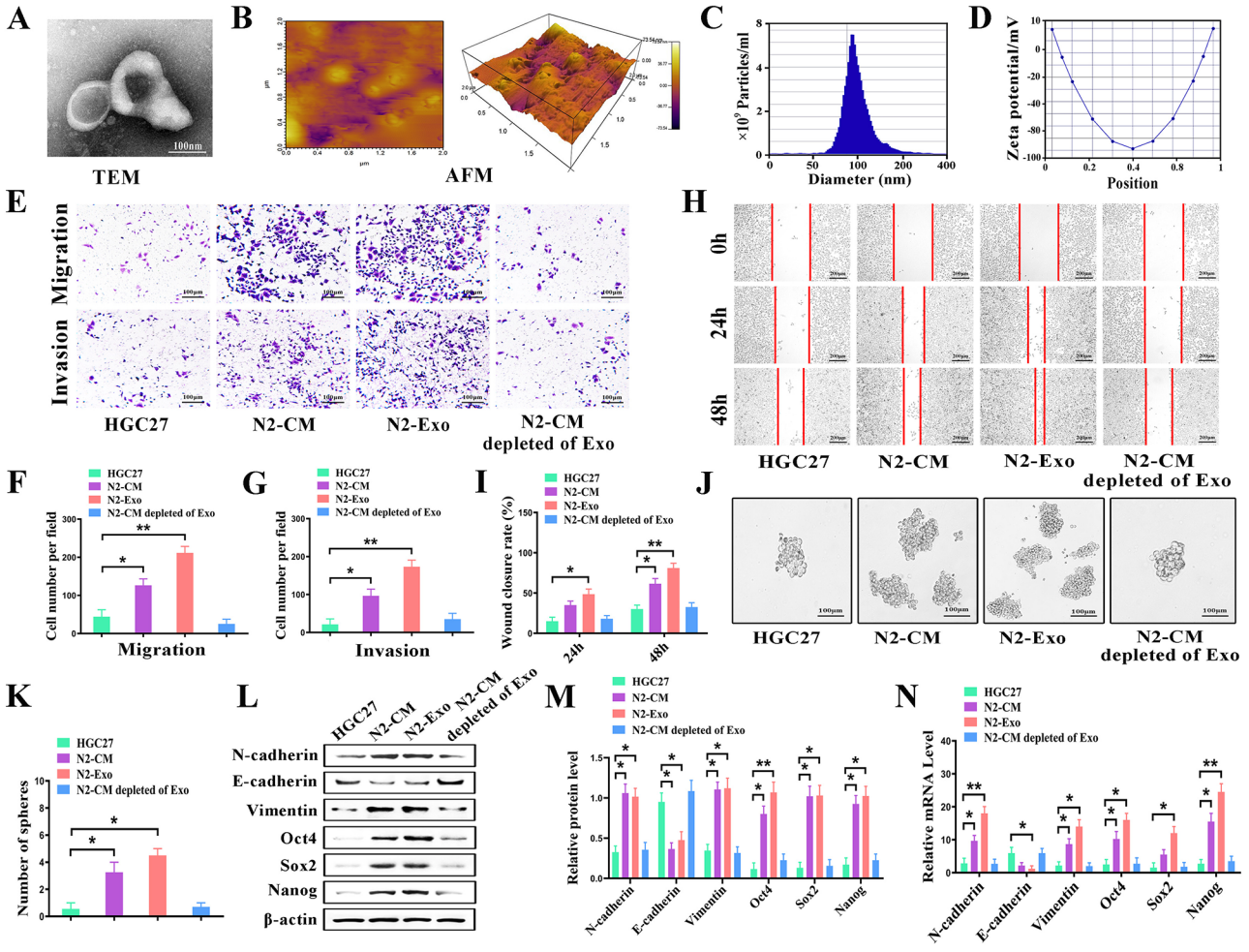

Fig. 1 N2-polarized neutrophils promote the metastatic potential and stemness of gastric cancer cells through exosomes. (**A-B**) TEM (**A**) and AFM (**B**) analyses of exosomes from N2-polarized neutrophils (N2-Exo). (**C-D**) NTA (**C**) and zeta-view (**D**) analyses of N2-Exo. (**E-G**) Transwell migration and matrigel invasion assays for gastric cancer cells treated with N2-CM and N2-Exo. Scale bars, 100 μm. (**H-I**) Wound healing assay for gastric cancer cells treated with N2-CM and N2-Exo. Scale bars, 200 μm. (**J-K**) Spheroid formation assay for gastric cancer cells treated with N2-CM and N2-Exo. Scale bars, 100 μm. (**L-N**) qRT-PCR and western blot assays for EMT and stemness-related gene (**N**) and protein (**L-M**) expression in gastric cancer cells treated with N2-CM and N2-Exo. *$P < 0.05$ and **$P < 0.01$

changes (Fig. 1H and I). In vitro tumor sphere formation assay showed that N2-Exo treatment enhanced the tumor sphere formation ability of gastric cancer cells (Fig. 1J and K). Western blot assays showed that N2-Exo treatment upregulated the expression of mesenchymal markers and stemness genes in gastric cancer cells (Fig. 1L and N, and Figure S3). These effects were also observed in other N2-Exo-treated gastric cancer cell lines (Figure S4). Taken together, these data indicate that N2-polarized neutrophils promote the metastatic potential and stemness of gastric cancer cells through exosomes.

N2-polarized neutrophils derived exosomes promote gastric cancer metastasis in vivo

To determine the effect of N2-Exo on cancer metastasis in vivo, we established a gastric cancer lung metastasis model by injecting HGC27 cells (stably transfected with a luciferase reporter gene) into nude mice via the tail vein. Eight days after the injection, N2-Exo was intravenously injected into the mice at 2-week intervals. Six weeks later, the mice were sacrificed, and lung metastasis nodules were examined (Fig. 2A). The infusion of N2-Exo significantly enhanced the intensity of the bioluminescence signals in the lungs of mice (Fig. 2B). H&E staining results further confirmed the increased number of metastatic foci in mouse lung tissues of the N2-Exo group (Fig. 2C and E). Furthermore, mice that received N2-Exo infusion presented a significantly shorter survival time than control mice (Fig. 2F). To further validate the effect of N2-Exo on cancer metastasis, we established a mouse peritoneal metastasis model following a similar procedure (Fig. 2G). We observed that N2-Exo infusion also increased the intensity of the bioluminescent signals in the peritoneum of mice (Fig. 2H). An increased number

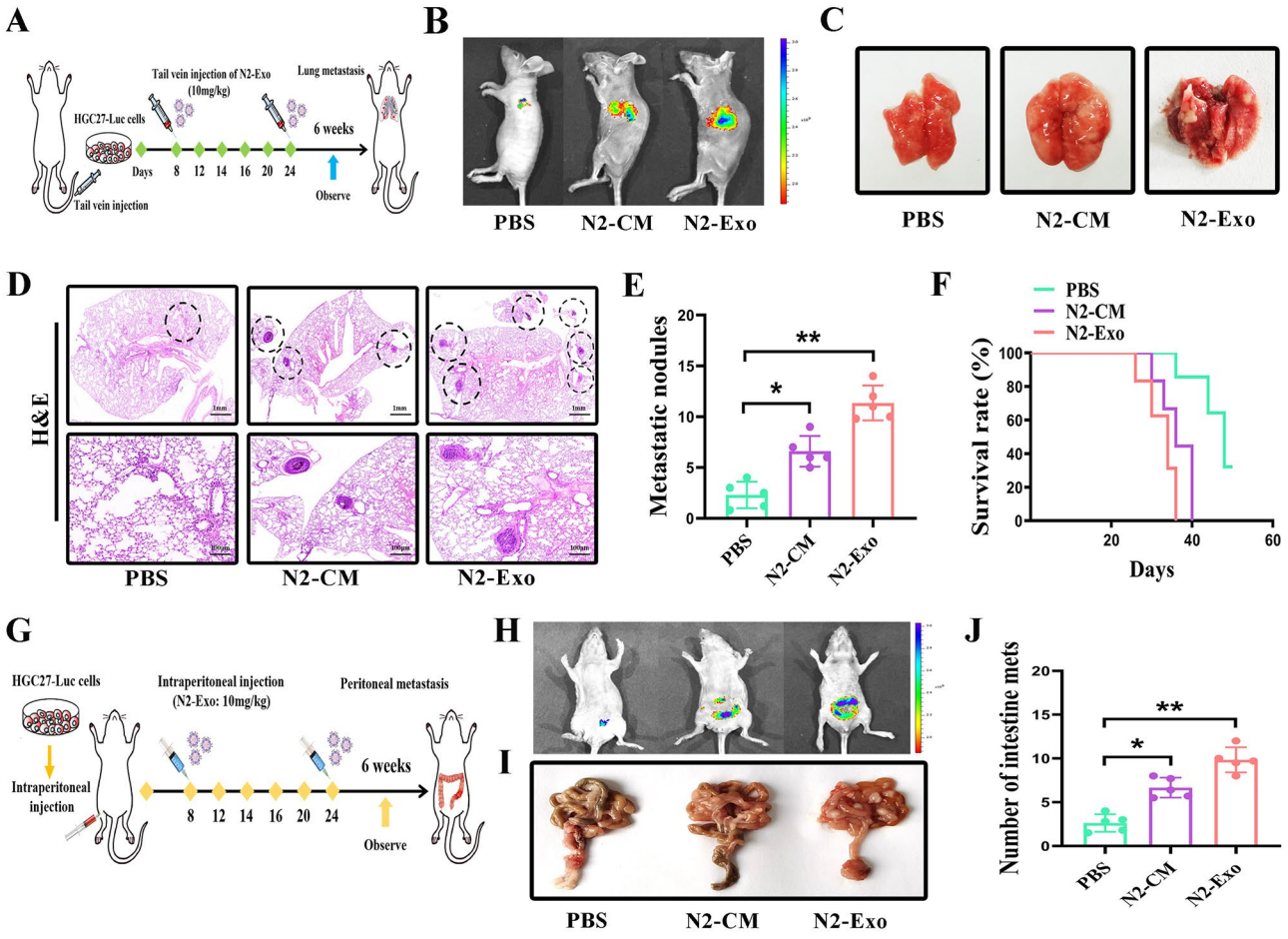

Fig. 2 N2-polarized neutrophils derived exosomes promote gastric cancer metastasis in vivo. (**A**) Flow chart of the procedure for evaluating the effects of N2-Exo on cancer metastasis in mouse tumor models. (**B**) The signal intensities of bioluminescent imaging in the lung tissues of indicated groups. (**C**) Lung tissues with metastatic nodules in the indicated groups. (**D**) H&E staining of lung tissues in the indicated groups. Top panel, scale bars, 1 mm. Bottom panel, scale bars, 100 μm. (**E**) The number of metastatic nodules in the lung tissues of indicated groups. (**F**) The survival time of mice in the indicated groups. (**G**) Schematic design for N2-Exo treatment in abdominal implantation tumor model. (**H**) The signal intensities of bioluminescent imaging in the peritoneum of indicated groups. (**I**) Intestine tissues with metastatic nodules in the indicated groups. (**J**) The number of metastatic nodules in the intestine tissues of indicated groups. **P* < 0.05 and ***P* < 0.01

of metastatic tumor nodules in intestinal tissues was also observed in the N2-Exo group (Fig. 2I and J). In summary, these data indicate that N2-Exo promotes gastric cancer metastasis and leads to poor prognosis.

N2-polarized neutrophils derived exosomes deliver miR-4745-5p and miR-3911 to gastric cancer cells

To further provide mechanistic insight into the roles of N2-Exo in cancer metastasis, we performed RNA sequencing for N2-Exo and found that N2-Exo were enriched in miRNAs (Fig. 3A), which was different from N1-Exo (Figure S5). The comparison between N2-Exo and exosomes from control neutrophils showed that several miRNAs are highly expressed in N2-Exo, including miR-4745-5p and miR-3911 (Fig. 3B). The list of the Top 10 differentially expressed miRNAs in N2-Exo is shown (Fig. 3C). The upregulation of miR-4745-5p and miR-3911 in GC-Exo-induced N2-polarized neutrophils was verified using qRT-PCR (Fig. 3D). Consistent with the RNA sequencing results, qRT-PCR results also showed that miR-4745-5p and miR-3911 expression was upregulated in N2-Exo compared to exosomes from control neutrophils (Fig. 3E). More importantly, miR-4745-5p and miR-3911 expression increased in gastric cancer cells after treatment with N2-Exo (Fig. 3F). To determine whether N2-Exo mediates the upregulation of miR-4745-5p and miR-3911 in gastric cancer cells via parallel transfer, we labeled miR-4745-5p and miR-3911 mimics with Cy3 and transfected neutrophils with the labeled miRNAs. The transfected neutrophils were co-cultured with gastric cancer cells in a transwell co-culture system (Fig. 3G), and the efficiency of transfection was detected by flow cytometry (Figure S6). Immunofluorescence results showed that Cy3-labeled miR-4745-5p

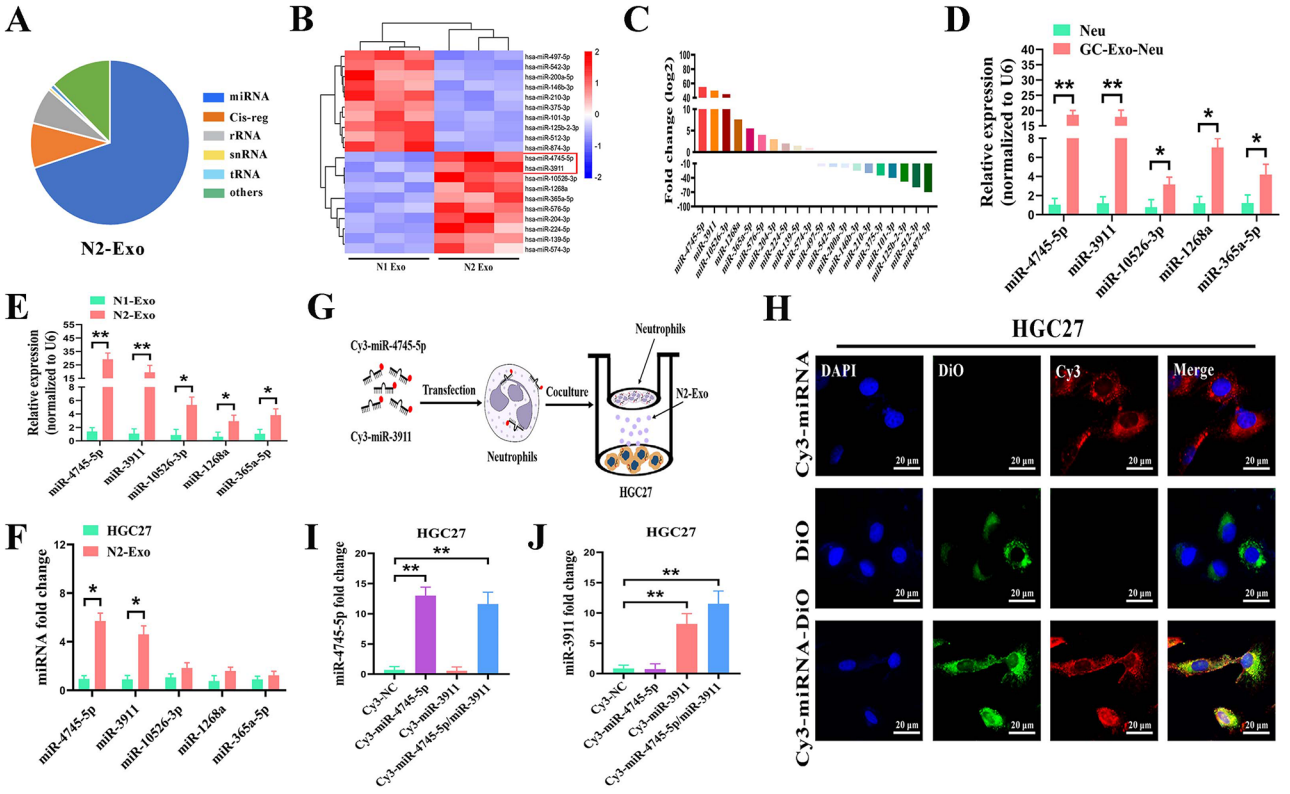

Fig. 3 N2-polarized neutrophils derived exosomes deliver miR-4745-5p and miR-3911 to gastric cancer cells. (**A**) RNA sequencing of N2-Exo. (**B**) Heatmap of Top10 differentially expressed miRNAs in N2-Exo. (**C**) Fold change of Top10 differentially expressed miRNAs in N2-Exo. (**D**) qRT-PCR analyses of the upregulated miRNAs in control and GC-Exo-induced, N2-polarized neutrophils. (**E**) qRT-PCR analyses of the upregulated miRNAs in N2-Exo. (**F**) qRT-PCR analyses of the upregulated miRNAs in gastric cancer cells (HGC27) treated with N2-Exo. (**G**) Neutrophils transfected with Cy3-labeled miR-4745-5p and miR-3911 were co-cultured with gastric cancer cells (HGC27) in a transwell co-culture system. (**H**) Gastric cancer cells were incubated with Dio-labeled exosomes from Cy3-miR-4745-5p and miR-3911 transfected neutrophils and observed under a fluorescent microscope. Scale bars, 20 μm. (**I-J**) qRT-PCR analyses of miR-4745-5p and miR-3911 expression in gastric cancer cells after co-culture with Cy3-miR-4745-5p and miR-3911 transfected neutrophils. **P* < 0.05 and ***P* < 0.01

and miR-3911 could be detected in co-cultured gastric cancer cells (Fig. 3H). Further qRT-PCR analyses confirmed the upregulation of miR-4745-5p and miR-3911 in co-cultured gastric cancer cells (Fig. 3I and J). Taken together, our data suggest that N2-polarized neutrophil-derived exosomes can directly deliver miR-4745-5p and miR-3911 to gastric cancer cells.

N2-polarized neutrophils derived exosomes promote gastric cancer metastasis via miR-4745-5p and miR-3911

Next, we determined the importance of N2-Exo derived miR-4745-5p and miR-3911 in cancer metastasis. We verified that miR-4745-5p and miR-3911 overexpression promoted, while their knockdown attenuated the proliferation, migration, and invasion of gastric cancer cells (Figure S7). We then collected exosomes from control and miR-4745-5p or miR-3911 knockdown N2-polarized neutrophils and tested their effects on the metastatic abilities of gastric cancer cells in vitro and in vivo. The results of transwell migration and matrigel invasion assays showed that the knockdown of either miR-4745-5p or miR-3911 greatly attenuated the promoting role of N2-Exo in the metastatic ability of gastric cancer cells in vitro (Fig. 4A and C). The results of cell colony formation and tumor sphere formation assays also showed that the knockdown of either miR-4745-5p or miR-3911 greatly reduced the enhancement of the tumor sphere formation ability of gastric cancer cells by N2-Exo (Figure S8). In vivo mouse lung metastasis models confirmed that the intensity of bioluminescent signals and the number of metastatic foci in the lungs of mice infused with miR-4745-5p or miR-3911 knockdown N2-Exo were significantly lower than those in mice infused with control N2-Exo (Fig. 4D and G). Furthermore, the number of metastatic tumor nodules in mouse intestinal tissues was also decreased by miR-4745-5p or miR-3911 knockdown in N2-Exo (Fig. 4H and I). To investigate the effect of N2-Exo derived miR-4745-5p and miR-3911 on tumor growth, HGC27 cells were injected subcutaneously in nude mice. The tumor sizes in miR-4745-5p or miR-3911 knockdown N2-Exo groups were smaller than those in control N2-Exo group (Figure S9). In summary,

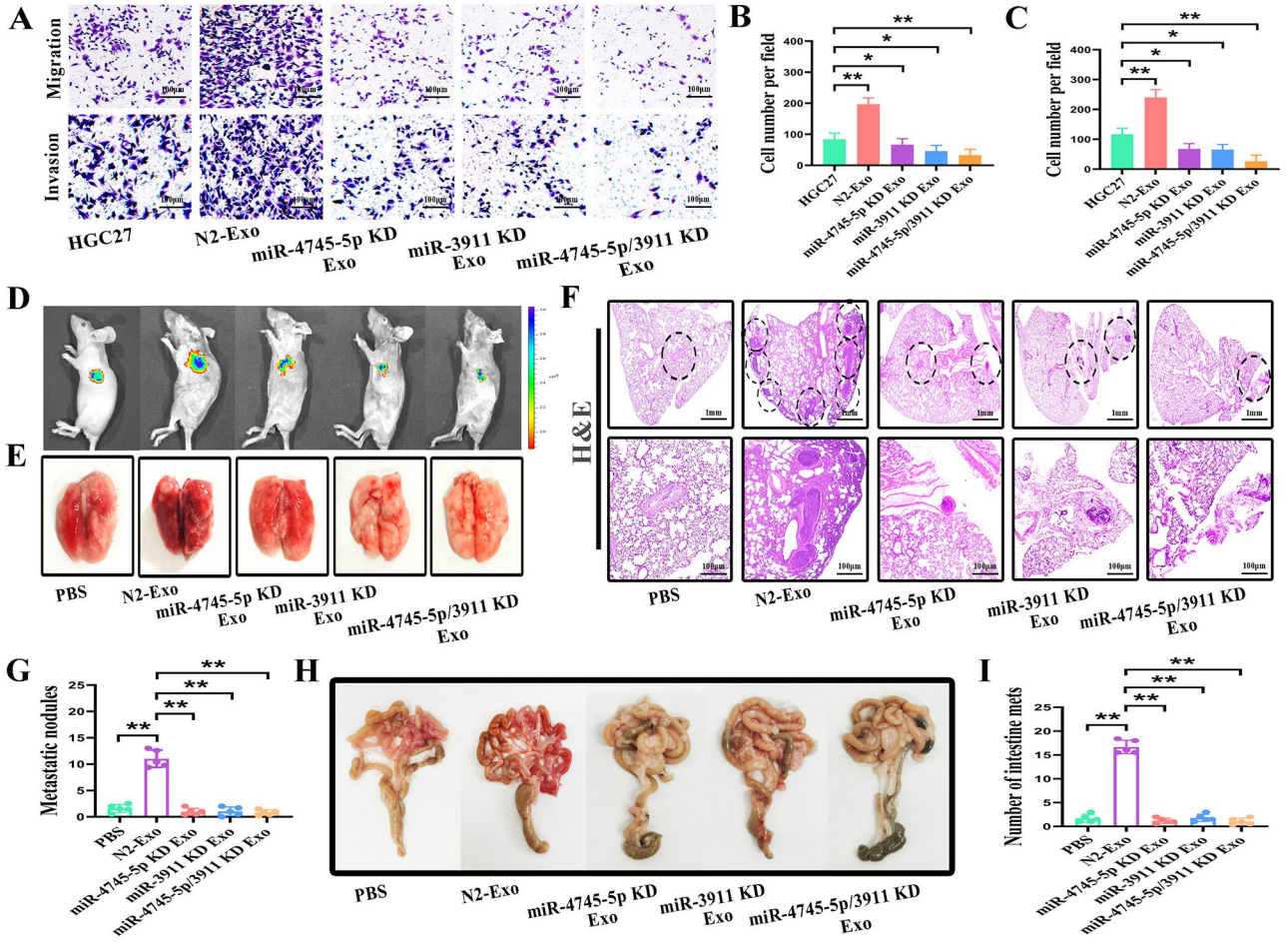

Fig. 4 N2-polarized neutrophils derived exosomes promote gastric cancer metastasis via exosomal miR-4745-5p/3911. (**A-C**) Transwell migration and matrigel invasion assays for gastric cancer cells (HGC27) treated with control or miR-4745-5p/3911 knockdown N2-Exo. Scale bars, 100 μm. (**D**) The signal intensities of bioluminescent imaging in the lung tissues of indicated groups. (**E**) Lung tissues with metastatic nodules in the indicated groups. (**F**) H&E staining of lung tissues in the indicated groups. Top panel, scale bars, 1 mm. Bottom panel, scale bars, 100 μm. (**G**) The number of metastatic nodules in the lung tissues of indicated groups. (**H**) Intestine tissues with metastatic nodules in the indicated groups. (**I**) The number of metastatic nodules in the intestine tissues of indicated groups. **P* < 0.05 and ***P* < 0.01

these results indicate that miR-4745-5p and miR-3911 are critical factors for N2-Exo to promote gastric cancer metastasis.

SLIT2 is a common target for miR-4745-5p and miR-3911 in gastric cancer cells

We then predicted the potential downstream target genes of miR-4745-5p or miR-3911 using bioinformatics and identified 17 common genes for both miRNAs (Fig. 5A). We focused on several cancer metastasis-related genes and paid particular interest to SLIT2 (slit guidance ligand 2) as it has been previously suggested as a tumor suppressor gene that restricts cancer metastasis [21]. We confirmed that miR-4745-5p or miR-3911 overexpression inhibited while their knockdown enhanced SLIT2 mRNA and protein expression in gastric cancer cells (Fig. 5B and E). The results of luciferase reporter assays showed that miR-4745-5p or miR-3911 overexpression inhibited while their knockdown enhanced the luciferase activity of wild-type, but not mutant, SLIT2 reporter genes in gastric cancer cells (Fig. 5F and J).

N2-polarized neutrophils derived exosomes promote gastric cancer metastasis via regulation of SLIT2

To determine whether N2-Exo promotes cancer metastasis by delivering miRNAs to regulate SLIT2 expression, we used N2-Exo to treat gastric cancer cells and found that SLIT2 expression was remarkably downregulated after treatment. In contrast, the expression of other predicted potential target genes of miR-4745-5p or miR-3911 showed minimal changes, suggesting that the regulation of SLIT2 by N2-Exo is specific (Fig. 6A). Western blotting results further confirmed the downregulation of SLIT2 protein by N2-Exo treatment in gastric cancer cells (Fig. 6B). Concurrent knockdown of miR-4745-5p or miR-3911 in gastric cancer cells antagonized the

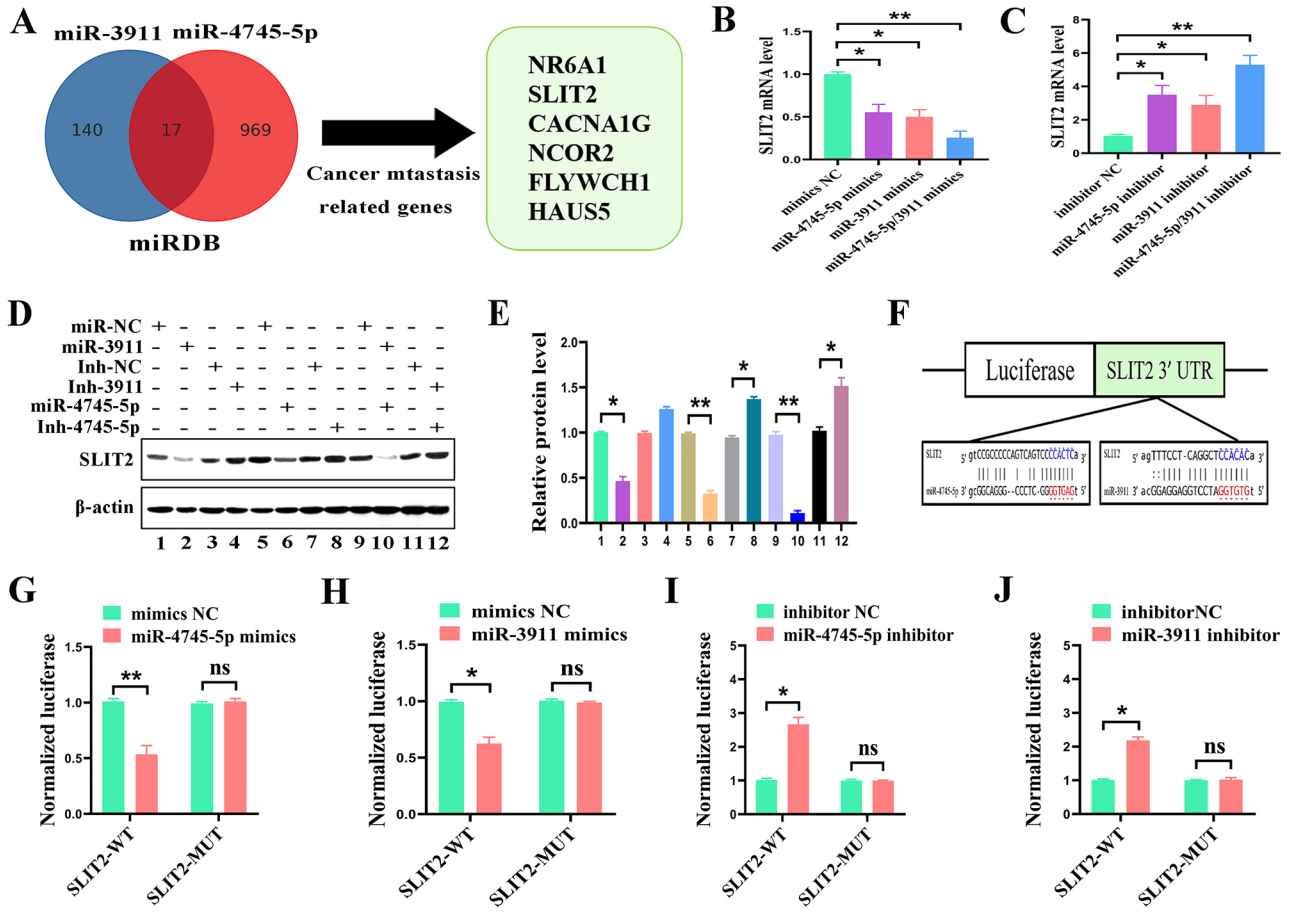

Fig. 5 SLIT2 is a common target for miR-4745-5p and miR-3911 in gastric cancer cells. (**A**) Bioinformatic analysis of the common target genes of miR-4745-5p and miR-3911. (**B-C**) qRT-PCR analyses of SLIT2 gene expression in miR-4745-5p and miR-3911 overexpressing (**B**) and knockdown (**C**) gastric cancer cells. (**D-E**) Western blot assays for SLIT2 protein expression in miR-4745-5p and miR-3911 overexpressing and knockdown gastric cancer cells. (**F**) The potential binding sites of miR-4745-5p and miR-3911 with SLIT2. (G-J) Luciferase reporter assays for SLIT2 reporter gene in miR-4745-5p and miR-3911 overexpressing (**G-H**) and knockdown (**I-J**) gastric cancer cells. **P* < 0.05 and ***P* < 0.01; ns, no significant change

inhibition of SLIT2 by N2-Exo treatment (Fig. 6C and D). The results of the luciferase reporter assay showed that N2-Exo treatment decreased the luciferase activity of the wild-type but not mutant SLIT2 reporter genes in gastric cancer cells (Fig. 6E), indicating that N2-Exo regulates SLIT2 via miR-4745-5p and miR-3911. To confirm this result, we treated HGC27 and MGC803 cells with exosomes collected from CAF, HUVEC, and N2 polarized neutrophils. We found that only N2-Exo could reduce SLIT2 protein level in gastric cancer cells (Figure S10). To further understand whether the regulation of SLIT2 by N2-Exo is critical for cancer metastasis, we performed rescue studies using adenovirus-mediated transfection of SLIT2 in gastric cancer cells. We found that the promotion of the metastatic ability of gastric cancer cells by N2-Exo was greatly attenuated by adenovirus-mediated transfection of SLIT2 (Ad-SLIT2) in vitro (Fig. 6F and H). Furthermore, in vivo mouse lung metastasis models confirmed that the intensity of bioluminescent signals and the number of metastatic foci in the lungs of mice infused with N2-Exo were significantly higher than those in mice infused with Ad-SLIT2 (Fig. 6I and L). We detected the expression level of SLIT2 in lung metastatic tissue and found a lower level of SLIT2 proteins in lung metastasis of N2-Exo treated mice (Fig. 6M). Taken together, these data suggest that N2-polarized neutrophils promote gastric cancer metastasis via exosomal miR-4745-5p/miR-3911-mediated regulation of SLIT2 expression.

Gastric cancer cells derived exosomes induce glucose metabolic reprogramming in neutrophils and subsequent upregulation of miR-4745-5p and miR-3911

Previously, we showed that gastric cancer cell-derived exosomes (GC-Exo) could induce N2 polarization of neutrophils [4]. To test the effect of gastric cancer cells on neutrophil glycolysis, we collected GC-Exo and treated neutrophils. qRT-PCR and western blot results showed that incubation with GC-Exo remarkably upregulated the expression levels of glycolysis-related genes in neutrophils, including PFKFB3, LDHA, HK-2, and PKM2

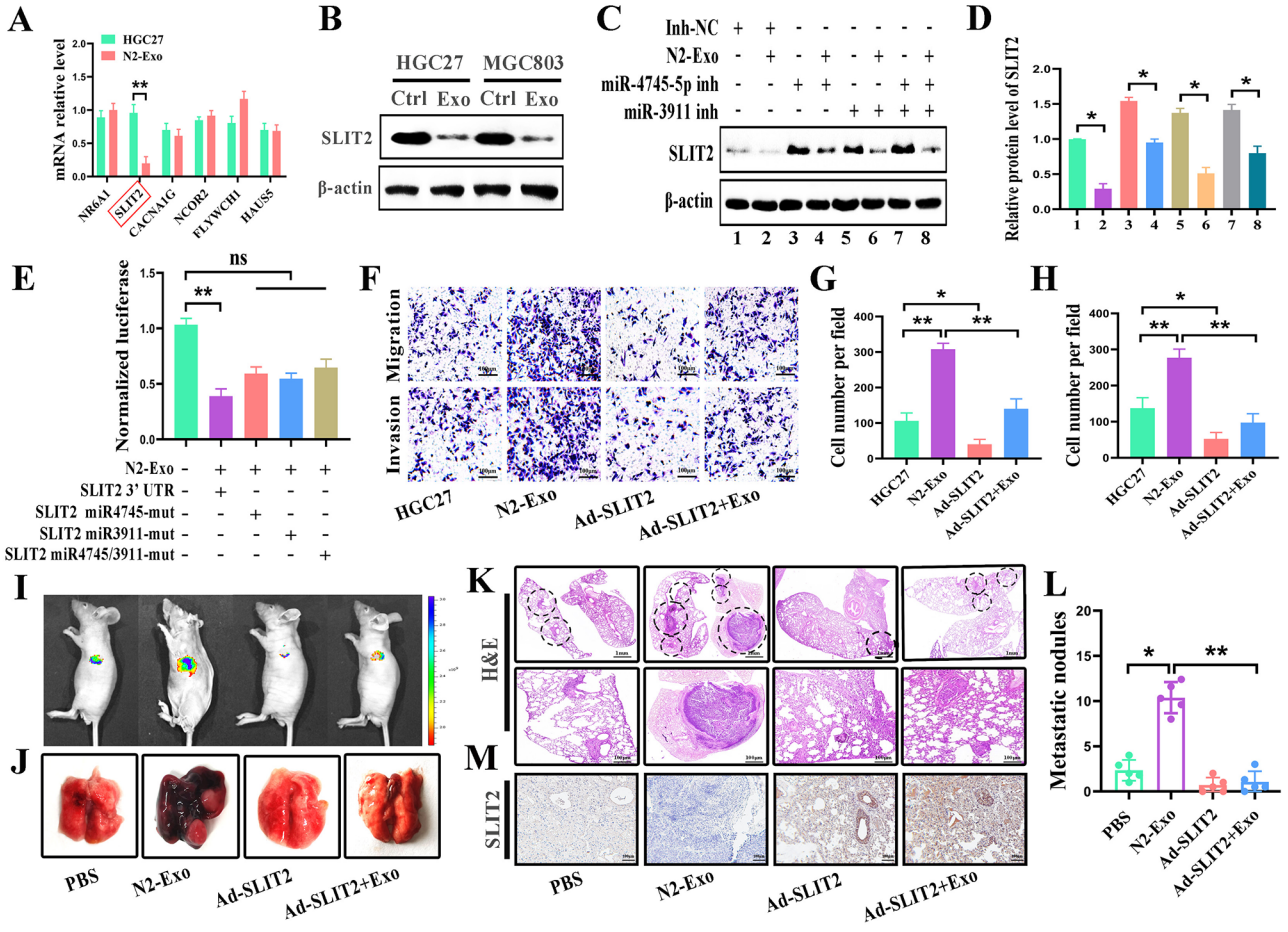

Fig. 6 N2-polarized neutrophils derived exosomes promote gastric cancer metastasis via regulation of SLIT2. (**A**) qRT-PCR analyses of SLIT2 gene expression in control and N2-Exo treated gastric cancer cells. (**B**) Western blot assays for SLIT2 protein expression in control and N2-Exo treated gastric cancer cells. (**C-D**) Western blot assays for SLIT2 protein expression in control and N2-Exo treated gastric cancer cells with or without miR-4745-5p and miR-3911 knockdown. (**E**) Luciferase reporter assays for N2-Exo-treated gastric cancer cells transfected with wild-type and mutant SLIT2 reporter gene vector. (**F-H**) Transwell migration and matrigel invasion assays for gastric cancer cells (HGC27) treated with N2-Exo and transfected with SLIT2 (Ad-SLIT2). Scale bars, 100 μm. (**I**) The signal intensities of bioluminescent imaging in the lung tissues of indicated groups. (**J**) Lung tissues with metastatic nodules in the indicated groups. (**K**) H&E staining of lung tissues in the indicated groups. Top panel, scale bars, 1 mm. Bottom panel, scale bars, 100 μm. (**L**) The number of metastatic nodules in the lung tissues of indicated groups. (**M**) SLIT2 staining in metastatic lung tissues. Scale bars, 100 μm. $^{*}P < 0.05$ and $^{**}P < 0.01$

(Fig. 7A and C). We also confirmed the vital roles of GC-Exo as the addition of GW4869 in the co-culture system attenuated the induction of neutrophil glycolysis in gastric cancer cells (Figure S11). Glucose uptake, lactate production, LDH activity, and ATP level assays showed that the glycolytic activity of neutrophils improved after treatment with GC-Exo (Fig. 7D and G). We revealed that HMGB1 is critical for the N2 polarization-inducing effect of GC-Exo. To determine whether GC-Exo induced neutrophil glycolysis through HMGB1, we prepared scramble control (si-Scr) and HMGB1 knockdown (si-HMGB1) GC-Exo and treated neutrophils with them. As shown in Fig. 7H and J, compared to si-Scr GC-Exo, the induction of glycolytic abilities in neutrophils by si-HMGB1 GC-Exo was apparently compromised, indicating that HMGB1 is the key factor that mediates the role of GC-Exo.

To further explore the glucose metabolic changes in N2-polarized neutrophils, we determined the impact of GC-Exo on the pentose phosphate pathway (PPP). As shown in Figure S14, the enzyme activities of glucose-6-phosphate dehydrogenase (G6PD) and NOX (NADPH oxidase) in neutrophils were significantly enhanced after GC-Exo treatment, suggesting that GC-Exo stimulation could activate the PPP pathway in neutrophils. Inhibition of NOX by diphenyleneiodonium chloride (DPI) decreased GC-Exo-induced upregulation of G6PD and miR-4745-5p/3911 (Figure S14).

Consistent with our previous study, GC-Exo mainly activated the NF-κB pathway to induce the upregulation of glycolysis-related genes and the increase of glycolytic activities in neutrophils, as pre-treatment with its inhibitor, Bay11-7082, reversed this effect (Figure S12). Moreover, the expression of miR-4745-5p and miR-3911 in

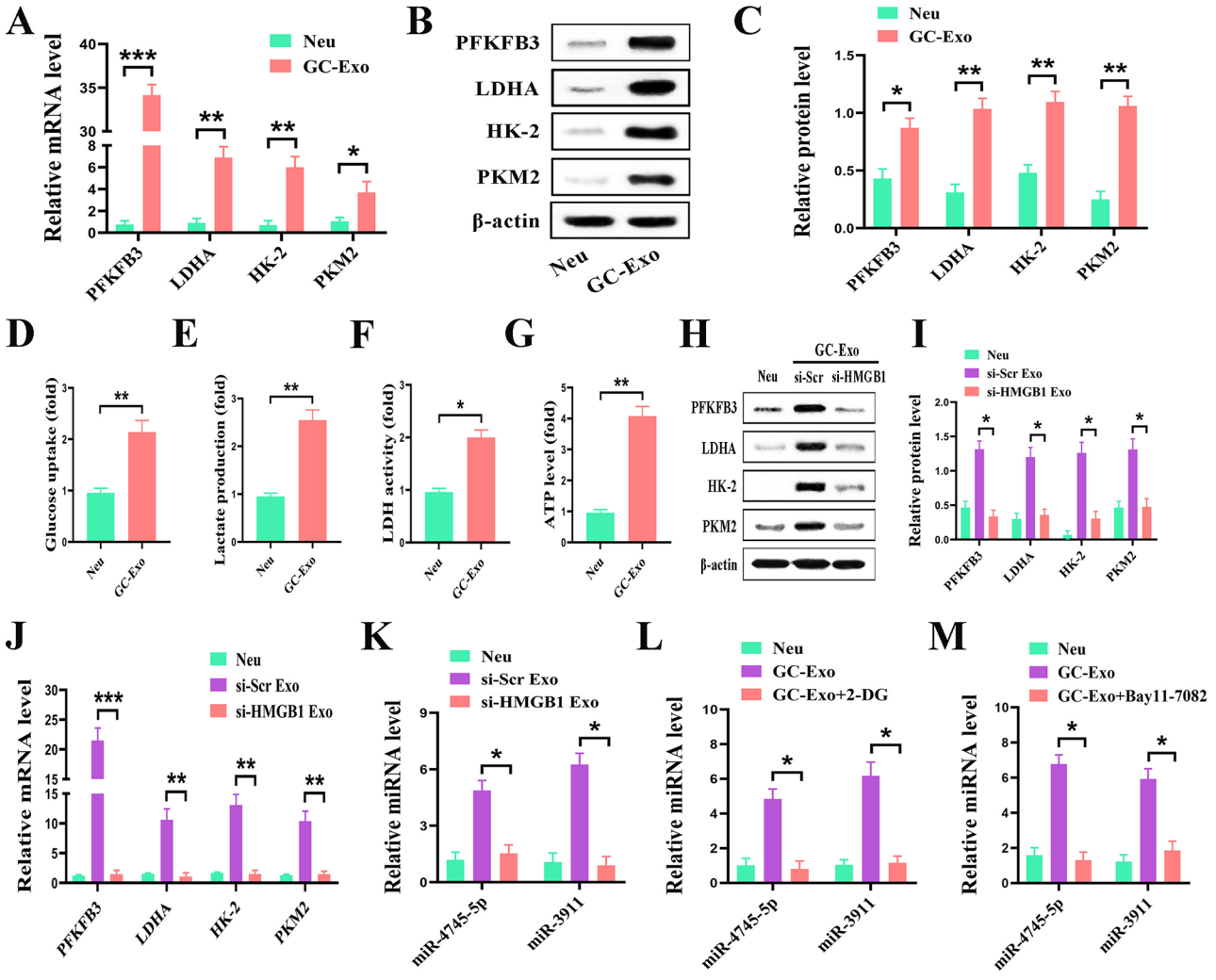

Fig. 7 Gastric cancer cells derived exosomes induce glycolysis-dependent upregulation of miR-4745-5p and miR-3911 in N2 polarized neutrophils. (**A-C**) qRT-PCR and western blot assays for glycolysis-related gene (**A**) and protein (**B-C**) expression in neutrophils and GC-Exo treated neutrophils. (**D-G**) Glucose uptake (**D**), lactate production (**E**), LDH activity (**F**), and ATP level (**G**) assays for neutrophils and GC-Exo induced neutrophils. (**H-I**) Western blot assays for glycolysis-related protein expression in neutrophils treated with scramble GC-Exo (si-Scr Exo) and HMGB1 knockdown GC-Exo (si-HMGB1 Exo). (**J**) qRT-PCR analyses of glycolysis-related gene expression in neutrophils treated with si-Scr Exo and si-HMGB1 Exo. (**K**) qRT-PCR analyses of miR-4745-5p and miR-3911 expression in neutrophils treated with si-Scr Exo and si-HMGB1 Exo. (**L**) The expressions of miR-4745-5p and miR-3911 in GC-Exo treated neutrophils with or without 2-DG. (**M**) qRT-PCR analyses of miR-4745-5p and miR-3911 expression in neutrophils treated with GC-Exo in the presence or absence of Bay11-7082. **P* < 0.05, ***P* < 0.01 and ****P* < 0.001

neutrophils treated with si-HMGB1 GC-Exo was significantly reduced (Fig. 7K). The miR-4745-5p and miR-3911 expression increased in GC-Exo-induced, N2-polarized neutrophils in a glycolysis-dependent manner, as pretreatment with 2-DG or Bay11-7082 reversed the upregulation of miR-4745-5p and miR-3911 (Fig. 7L and M). N2-polarized neutrophils induced by GC-Exo have been reported to promote gastric cancer cell migration and invasion. To understand the role of glycolysis in this process, we collected CM from GC-Exo-induced, N2-polarized neutrophils (N2-CM) in the presence or absence of the glycolysis inhibitor 2-DG. We found that 2-DG pretreatment significantly inhibited the promotion of gastric cancer cell migration and invasion by CM from GC-Exo-treated neutrophils (Figure S13). In summary, these findings indicate that gastric cancer cells induce glycolysis-dependent N2 polarization of neutrophils through exosomal HMGB1 and activation of the NF-κB pathway.

The expression levels of miR-4745-5p and miR-3911 are elevated in N2-polarized neutrophils derived exosomes from serum of gastric cancer patients

Finally, we aimed to clarify the clinical value of N2-polarized neutrophils in gastric cancer. Immunohistochemical staining results showed that gastric cancer patients with metastasis were prone to have a high number of

infiltrating neutrophils and low levels of SLIT2 expression in the tumor tissues compared to patients without metastasis (Fig. 8A and B, and Figure S15). We also observed that the expression levels of miR-4745-5p and miR-3911 were higher in gastric cancer tissues than in matched normal tissues, and their levels were negatively associated with that of SLIT2 in gastric cancer tissues (Figure S16).

Previous studies indicate that high-density neutrophils (HDNs) and low-density neutrophils (LDNs) in the circulation of cancer patients may represent N1 and N2 neutrophils, respectively [22]. Then, we isolated HDNs and LDNs from peripheral blood of gastric cancer patients by using density gradient centrifugation and verified their morphology by wright-giemsa staining (Figures S17A and S17B). We found that LDNs expressed higher levels of miR-4745-5p/3911 than HDNs (Figure S17C).

We collected serum samples from healthy controls (HC), patients with benign gastric diseases (BGD), and patients with gastric cancer (GC) and isolated the total exosomes. qRT-PCR results showed that the expression levels of miR-4745-5p and miR-3911 were elevated in the GC group compared to those in the HC and BGD groups (Fig. 8C and D). ROC curves showed that the area under curve (AUC) for miR-4745-5p and miR-3911 to discriminate GC from HC were 0.827 and 0.836, respectively. The combination of miR-4745-5p and miR-3911 increased the AUC to 0.912. The AUC for miR-4745-5p and miR-3911 to discriminate GC from BGD were 0.738 and 0.786, respectively. The combination of miR-4745-5p and miR-3911 increased the AUC to 0.863 (Fig. 8E and F). Recently, we developed a rapid and sensitive droplet digital PCR (ddPCR)-based method to detect neutrophil exosomal miRNAs in the serum of patients with gastric

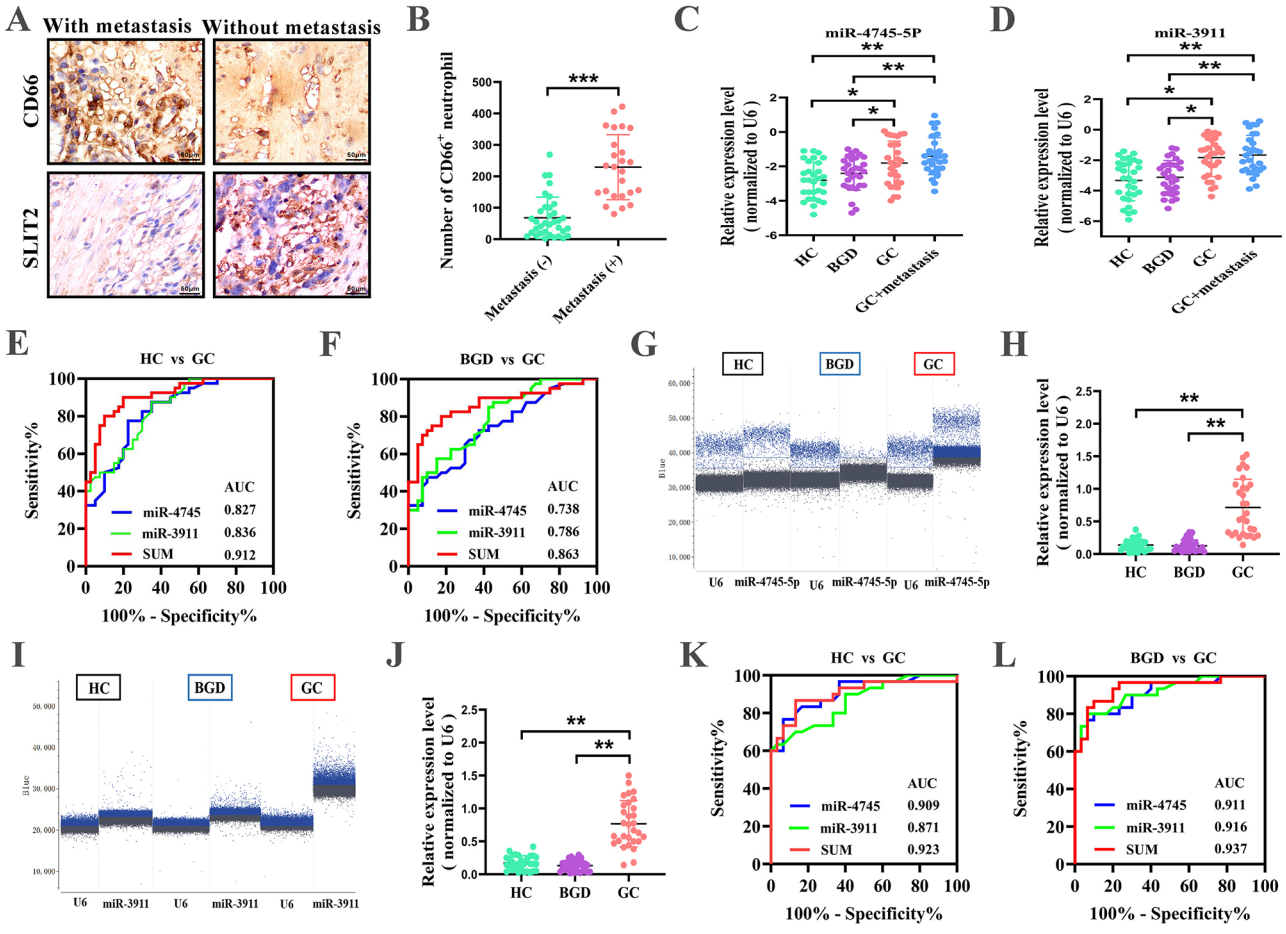

Fig. 8 Circulating levels of miR-4745-5p and miR-3911 are elevated in N2-polarized neutrophils derived exosomes from gastric cancer patients. (**A-B**) Immunohistochemical staining of CD66 and SLIT2 in gastric cancer tissues with or without metastasis ($n = 25$). Scale bars, 100 μm. (**C-D**) qRT-PCR analyses of miR-4745-5p (**C**) and miR-3911 (**D**) expression in serum samples from healthy controls (HC), benign gastric diseases (BGD), and gastric cancer (GC) patients ($n = 30$). (**E-F**) The area under curve (AUC) to distinguish GC from GC (**E**) and BGD (**F**) groups. (**G-J**) The expression of miR-4745-5p (**G**) and miR-3911 (**I**) in serum samples ($n = 30$) from HC, BGD, GC patients detected by droplet digital PCR (ddPCR) and the statistical analysis result (**H** and **J**). (**K-L**) The area under curve (AUC) to distinguish GC from GC (**K**) and BGD (**L**) groups for ddPCR analyses of miR-4745-5p and miR-3911 expression in serum neutrophil exosomes. *$P < 0.05$, **$P < 0.01$ and ***$P < 0.001$. All samples are providing from our own source of patient samples

cancer [23]. We applied this method to the detection of miR-4745-5p and miR-3911 in neutrophil-derived exosomes using serum samples from HC, BGD, and GC groups. The ddPCR detection results showed that the expression levels of miR-4745-5p and miR-3911 were elevated in the GC group compared to those in the HC and BGD groups (Fig. 8G and J). ROC curves showed that the AUC for miR-4745-5p and miR-3911 in discriminating GC from HC and BGD could be further increased to 0.923 and 0.937 when combined (Fig. 8K and L). In summary, these data suggest that the expression levels of miR-4745-5p and miR-3911 in neutrophil-derived exosomes may serve as potential biomarkers for gastric cancer.

Discussion

In this study, we present the first evidence that N2-polarized neutrophils promote gastric cancer progression via exosomes. We reported that gastric cancer cells induced N2 polarization of neutrophils in a glucose metabolism reprogramming-dependent manner, which upregulated the expression of miR-4745-5p and miR-3911 in neutrophils and their release via exosomes. N2-polarized neutrophil exosomes derived miR-4745-5p and miR-3911 could be efficiently internalized by gastric cancer cells, leading to downregulation of SLIT2 gene and enhancement of metastatic abilities of gastric cancer cells in vitro and in vivo. We confirmed that the tumor-promoting role of N2-polarized neutrophil-derived exosomes is dependent on the parallel transfer of miR-4745-5p and miR-3911 and that SLIT2 overexpression could antagonize the role of N2-Exo. Our findings are consistent with previous reports showing that N2 neutrophils promote the metastasis of lung and breast cancers via exosomes [17, 18], indicating that N2-polarized neutrophil-derived exosomes may be a common mechanism for their tumor-promoting roles. Our findings, together with those from other studies, add another layer of information on the intricate interactions between TANs and tumor cells in the TME.

Metabolic reprogramming is closely associated with neutrophil function in several diseases. For instance, in human psoriasis, a metabolic shift toward glycolysis has been observed in $CXCR4^{hi}$ neutrophils, which promotes vascular permeability and skin inflammatory responses [24]. Recent studies have linked the hyperactivated glycolytic activity of neutrophils with their pro-tumor functions [25, 26]. Using single-cell RNA sequencing, Wang et al. have identified a heterogeneous pro-tumor subset of neutrophils associated with poor prognosis in the TME of pancreatic ductal adenocarcinoma (PDAC) [26]. This subpopulation is characterized by hyperactivated glycolytic activity, and the glycolytic switch promotes pro-tumor functions in neutrophils. It has been revealed that the cellular metabolic switch regulates the pro-tumor functions of monocytes in the TME of human hepatocellular carcinoma [27]. The promotion of glycolysis in cancer cells by neutrophils has been previously proposed [16, 28], but the regulation of glycolysis in neutrophils by tumors has not been well studied. The activation of PPP pathway has been linked to neutrophil N2 polarization [29]. We showed that gastric cancer cell-derived exosomes induced activation of glycolysis and PPP pathways in neutrophils. We previously demonstrated that gastric cancer cell-derived exosomes induced N2 polarization of neutrophils via exosomal HMGB1-mediated activation of the NF-κB pathway in these cells [4]. Herein, we further showed that the induction of glycolysis and PPP pathway activation is critical for the upregulation of miRNAs in N2 polarized neutrophils, suggesting a metabolic reprogramming-dependent mechanism for the pro-tumor function of neutrophils in the TME.

Recent studies have indicated an important role of miRNAs in the regulation and function of neutrophils [30]. These miRNAs are transported by neutrophil-derived exosomes, causing tissue inflammation in many diseases. The activation of neutrophils with various inflammatory stimuli induces the release of exosomes enriched in miR-142-3p and miR-451, which could target endothelial cells to trigger an inflammatory cascade and induce direct vascular damage [31]. In non-alcoholic steatohepatitis (NASH), neutrophil-derived miR-223-enriched exosomes are preferentially taken up by hepatocytes, which are dependent on low-density lipoprotein receptors on hepatocytes and apolipoprotein E on neutrophil-derived exosomes, to inhibit hepatic inflammatory and fibrogenic gene expression, limiting NASH progression in obese mice [32]. In sepsis-related acute lung injury (ALI), TNF-α-stimulated neutrophils release exosomes that contain miR-30d-5p to target SOCS-1 (suppressor of cytokine signaling) and SIRT1 (sirtuin 1) in macrophages, priming pyroptosis by upregulating NLRP3 inflammasome expression through the NF-κB signaling pathway [33]. The role of exosomal miRNAs derived from N2 neutrophils in cancer progression is not well understood. Upon chronic nicotine exposure, STAT3-activated N2-neutrophils secrete exosomal miR-4466 to promote stemness and metabolic switching via the SKI/SOX2/CPT1A axis in tumor cells in the brain, thereby enhancing metastasis [15]. Wang et al. have sequenced the miRNA profile of exosomes from TGF-β1-induced N2 neutrophils and identified upregulation of miR-4780 and downregulation of miR-3938 in N2 neutrophils [34]. Herein, we reported that exosomes from N2 neutrophils (induced by GC-Exo) display a distinct miRNA profile compared to their control counterparts. In particular, we identified miR-4745-5p and miR-3911 as the most upregulated miRNAs in N2-Exo and confirmed that they are critical factors

that mediate the tumor-promoting role of N2-Exo, further proving the importance of exosomal miRNAs from neutrophils in disease progression.

The biological roles of miR-4745-5p and miR-3911 in cancer have not yet been reported. We found that miR-4745-5p and miR-3911 both target SLIT2 to inhibit its expression. The SLIT family and its receptor ROBO family were originally identified in the nervous system, where they play a crucial role in the directed migration of neuronal cells. The migration of tumor and neuronal cells shares common signaling pathways. The function of the SLIT2/ROBO axis in cancer seems to be controversial, as SLIT2 has been shown to perform both promoting and inhibiting roles in different cancers, depending on the cancer type, cell type, and cellular context. It has been reported that deleting endothelial SLIT2 suppressed metastatic dissemination, whereas deletion of tumoral SLIT2 enhances metastatic progression in mouse models of breast and lung cancer [35]. A recent study that uses in vivo genome-wide CRISPR knockout identifies SLIT2 knockout circulating tumor cells (CTCs) are highly metastatic [21]. SLIT2 is inactivated in multiple types of cancers, mainly due to promoter hypermethylation or loss of heterozygosity (LOH). The mRNA and protein levels of SLIT2 are lower in GC tissues than those in the adjacent normal tissues [36]. Previous studies suggest that SLIT2 knockdown promotes the growth and motility of gastric cancer cells by activating the AKT/β-catenin pathway [37]. Our data showed that SLIT2 expression in cancer cells might also be regulated by exosomal miRNAs from N2 TANs, indicating a new mode of SLIT2 regulation by microenvironmental cues.

Aberrant expression of miRNAs in neutrophil-derived exosomes has been previously observed in several inflammatory diseases. For instance, Li et al. have sequenced the profile of miRNAs in peripheral blood neutrophil exosomes of diffuse cutaneous systemic sclerosis (dSSc), a systemic autoimmune disease with skin fibrosis, and have identified 22 dysregulated miRNAs (such as the upregulation of miR-1268a) in neutrophil exosomes of dSSc patients [38]. In addition, miR-142-3p and miR-451 levels are markedly increased in kidney biopsies from patients with active ANCA-associated vasculitis, a severe autoimmune disease associated with neutrophil-induced microvascular damage [31]. MiR-150-5p from neutrophil-derived exosomes is upregulated in the blood samples of sepsis patients with sepsis-induced cardiomyopathy. In particular, coupled with other indicators such as NT-pro BNP, LVEF, and SOFA score, it is found to be independent predictor of septic cardiomyopathy (with an AUC of 0.941) [39]. We recently developed a rapid isolation method for neutrophil exosomes and ddPCR-based detection of their derived miRNAs [23]. We showed that the expression levels of miR-4745-5p and miR-3911 were elevated in neutrophil exosomes from the serum samples of gastric cancer patients compared to those from healthy controls and patients with benign gastric disease, which may represent a novel biomarker for GC diagnosis.

In conclusion, we demonstrated that gastric cancer cells induced N2 polarization of neutrophils by glucose metabolism reprogramming. N2-polarized neutrophils promoted gastric cancer metastasis through exosomal miR-4745-5p/3911-mediated inhibition of SLIT2 expression in gastric cancer cells (Fig. 9). Our findings not only reveal a new mechanism for the pro-tumor roles of N2 TANs in cancer but also provide a potential diagnostic biomarker for gastric cancer.

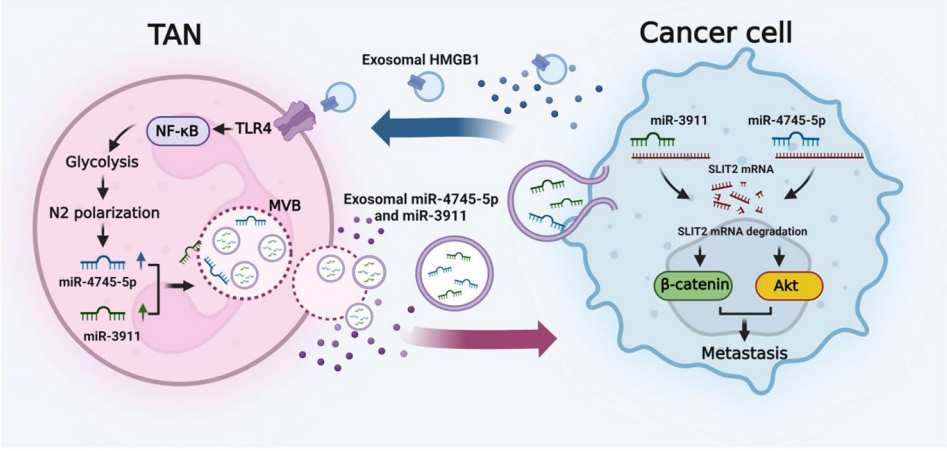

Fig. 9 Proposed model of the role of exosomes-mediated crosstalk between N2 TANs and gastric cancer cells in gastric cancer metastasis. Gastric cancer cells induce the N2 polarization of neutrophils via a glycolysis-dependent manner. In turn, N2-polarized neutrophils promote gastric cancer metastasis through exosomal miR-4745-5p/3911-mediated inhibition of SLIT2 expression in gastric cancer cells. Serum neutrophil exosomal miR-4745-5p/3911 represents a novel biomarker for GC diagnosis

Supplementary Information

The online version contains supplementary material available at https://doi.org/10.1186/s12943-024-02116-6.

Supplementary Material 1

Supplementary Material 2

Acknowledgements
We would like to thank the members of the Zhang Lab for their helpful discussions and technical support.

Author contributions
JZ, JG, and XZ: Conception and design. JZ, DY, CJ, and MW: Development of methodology. MF, YQ, XZ, and RJ: data acquisition. JZ, CJ, JG, and XZ analyzed and interpreted the data. JZ, JG, and XZ wrote, reviewed, and revised the manuscript. CL, JG and XZ: Administrative, technical, or material support. XZ: Study supervision.

Funding
This work was supported by the National Natural Science Foundation of China (82372909, 81972310), Distinguished Young Scholar Project of Jiangsu Province (BK20200043), Non-profit Central Research Institute Fund of the Chinese Academy of Medical Sciences (NLDTG2020002), Nantong Science and Technology Bureau Project (JCZ2023005), Zhenjiang Policy Guidance Program for International Science and Technology Cooperation (GJ2023015), China Postdoctoral Science Foundation (2023M741431), Zhenjiang Science and Technology Innovation Fund (SH2023048) and Postgraduate Research & Practice Innovation Program of Jiangsu Province (KYCX21_3405, KYCX22_3713, KYCX23_3762).

Data availability
No datasets were generated or analysed during the current study.

Declarations

Ethics approval and consent to participate
The use of clinical samples was approved by the Ethics Committee of Jiangsu University, and informed consent was obtained from all patients.

Consent for publication
All authors are aware of and agree with the content of the paper and are listed as co-authors of the paper.

Competing interests
The authors declare no competing interests.

Received: 2 July 2024 / Accepted: 5 September 2024
Published online: 13 September 2024

References

1. Hedrick CC, Malanchi I. Neutrophils in cancer: heterogeneous and multifaceted. Nat Rev Immunol. 2022;22(3):173–87.
2. Shaul ME, Fridlender ZG. Tumour-associated neutrophils in patients with cancer. Nat Rev Clin Oncol. 2019;16(10):601–20.
3. Jaillon S, Ponzetta A, Di Mitri D, Santoni A, Bonecchi R, Mantovani A. Neutrophil diversity and plasticity in tumour progression and therapy. Nat Rev Cancer. 2020;20(9):485–503.
4. Zhang X, Shi H, Yuan X, Jiang P, Qian H, Xu W. Tumor-derived exosomes induce N2 polarization of neutrophils to promote gastric cancer cell migration. Mol Cancer. 2018;17(1):146.
5. Xiong S, Dong L, Cheng L. Neutrophils in cancer carcinogenesis and metastasis. J Hematol Oncol. 2021;14(1):173.
6. Kalluri R, McAndrews KM. The role of extracellular vesicles in cancer. Cell. 2023;186(8):1610–26.
7. Yang Y, Guo Z, Chen W, Wang X, Cao M, Han X, et al. M2 macrophage-derived exosomes promote angiogenesis and growth of pancreatic ductal adenocarcinoma by targeting E2F2. Mol Therapy: J Am Soc Gene Therapy. 2021;29(3):1226–38.
8. Grunberg N, Pevsner-Fischer M, Goshen-Lago T, Diment J, Stein Y, Lavon H, et al. Cancer-associated fibroblasts promote aggressive gastric cancer phenotypes via heat shock factor 1-mediated secretion of extracellular vesicles. Cancer Res. 2021;81(7):1639–53.
9. Marki A, Ley K. The expanding family of neutrophil-derived extracellular vesicles. Immunol Rev. 2022;312(1):52–60.
10. Forrest OA, Dobosh B, Ingersoll SA, Rao S, Rojas A, Laval J, et al. Neutrophil-derived extracellular vesicles promote feed-forward inflammasome signaling in cystic fibrosis airways. J Leukoc Biol. 2022;112(4):707–16.
11. Zhang XY, Chen ZC, Li N, Wang ZH, Guo YL, Tian CJ, et al. Exosomal transfer of activated neutrophil-derived lncRNA CRNDE promotes proliferation and migration of airway smooth muscle cells in asthma. Hum Mol Genet. 2022;31(4):638–50.
12. Genschmer KR, Russell DW, Lal C, Szul T, Bratcher PE, Noerager BD et al. Activated PMN exosomes: pathogenic entities causing matrix destruction and disease in the lung. Cell. 2019;176(1–2):113 – 26.e15.
13. Gomez I, Ward B, Souilhol C, Recarti C, Ariaans M, Johnston J, et al. Neutrophil microvesicles drive atherosclerosis by delivering miR-155 to atheroprone endothelium. Nat Commun. 2020;11(1):214.
14. Bao W, Xing H, Cao S, Long X, Liu H, Ma J, et al. Neutrophils restrain sepsis associated coagulopathy via extracellular vesicles carrying superoxide dismutase 2 in a murine model of lipopolysaccharide induced sepsis. Nat Commun. 2022;13(1):4583.
15. Rubenich DS, Omizzollo N, Szczepański MJ, Reichert TE, Whiteside TL, Ludwig N, et al. Small extracellular vesicle-mediated bidirectional crosstalk between neutrophils and tumor cells. Cytokine Growth Factor Rev. 2021;61:16–26.
16. Li B, Zhu L, Lu C, Wang C, Wang H, Jin H, et al. circNDUFB2 inhibits non-small cell lung cancer progression via destabilizing IGF2BPs and activating anti-tumor immunity. Nat Commun. 2021;12(1):295.
17. Tyagi A, Wu SY, Sharma S, Wu K, Zhao D, Deshpande R, et al. Exosomal miR-4466 from nicotine-activated neutrophils promotes tumor cell stemness and metabolism in lung cancer metastasis. Oncogene. 2022;41(22):3079–92.
18. Ou B, Liu Y, Gao Z, Xu J, Yan Y, Li Y, et al. Senescent neutrophils-derived exosomal piRNA-17560 promotes chemoresistance and EMT of breast cancer via FTO-mediated m6A demethylation. Cell Death Dis. 2022;13(10):905.
19. Peng K, Wu Z, Feng Z, Deng R, Ma X, Fan B, et al. A highly integrated digital PCR system with on-chip heating for accurate DNA quantitative analysis. Biosens Bioelectron. 2024;253:116167.
20. Xu Q, Li J, Zhang Z, Yang Q, Zhang W, Yao J, et al. Precise determination of reaction conditions for accurate quantification in digital PCR by real-time fluorescence monitoring within microwells. Biosens Bioelectron. 2024;244:115798.
21. Xia F, Ma Y, Chen K, Duong B, Ahmed S, Atwal R, et al. Genome-wide in vivo screen of circulating tumor cells identifies SLIT2 as a regulator of metastasis. Sci Adv. 2022;8(35):eabo7792.
22. Sagiv Jitka Y, Michaeli J, Assi S, Mishalian I, Kisos H, Levy L, et al. Phenotypic diversity and plasticity in circulating neutrophil subpopulations in cancer. Cell Rep. 2015;10(4):562–73.
23. Yu D, Zhang J, Wang M, Ji R, Qian H, Xu W, et al. Exosomal miRNAs from neutrophils act as accurate biomarkers for gastric cancer diagnosis. Clin Chim Acta. 2024;554:117773.
24. Chen J, Bai Y, Xue K, Li Z, Zhu Z, Li Q, et al. CREB1-driven CXCR4(hi) neutrophils promote skin inflammation in mouse models and human patients. Nat Commun. 2023;14(1):5894.
25. Ng MSF, Kwok I, Tan L, Shi C, Cerezo-Wallis D, Tan Y, et al. Deterministic reprogramming of neutrophils within tumors. Sci (New York NY). 2024;383(6679):eadf6493.
26. Wang L, Liu Y, Dai Y, Tang X, Yin T, Wang C, et al. Single-cell RNA-seq analysis reveals BHLHE40-driven pro-tumour neutrophils with hyperactivated glycolysis in pancreatic tumour microenvironment. Gut. 2023;72(5):958–71.
27. Chen DP, Ning WR, Jiang ZZ, Peng ZP, Zhu LY, Zhuang SM, et al. Glycolytic activation of peritumoral monocytes fosters immune privilege via the PFKFB3-PD-L1 axis in human hepatocellular carcinoma. J Hepatol. 2019;71(2):333–43.
28. Ou B, Liu Y, Yang X, Xu X, Yan Y, Zhang J. C5aR1-positive neutrophils promote breast cancer glycolysis through WTAP-dependent m6A methylation of ENO1. Cell Death Dis. 2021;12(8):737.
29. Maus KD, Stephenson DJ, Macknight HP, Vu NT, Hoeferlin LA, Kim M, et al. Skewing cPLA(2)α activity toward oxoeicosanoid production promotes

neutrophil N2 polarization, wound healing, and the response to sepsis. Sci Signal. 2023;16(793):eadd6527.
30. Garley M, Nowak K, Jabłońska E. Neutrophil microRNAs. Biological reviews of the Cambridge Philosophical Society. 2023.
31. Glémain A, Néel M, Néel A, André-Grégoire G, Gavard J, Martinet B, et al. Neutrophil-derived extracellular vesicles induce endothelial inflammation and damage through the transfer of miRNAs. J Autoimmun. 2022;129:102826.
32. He Y, Rodrigues RM, Wang X, Seo W, Ma J, Hwang S et al. Neutrophil-to-hepatocyte communication via LDLR-dependent mir-223-enriched extracellular vesicle transfer ameliorates nonalcoholic steatohepatitis. J Clin Investig. 2021;131(3).
33. Jiao Y, Zhang T, Zhang C, Ji H, Tong X, Xia R, et al. Exosomal miR-30d-5p of neutrophils induces M1 macrophage polarization and primes macrophage pyroptosis in sepsis-related acute lung injury. Crit Care (London England). 2021;25(1):356.
34. Wang L, Yang J, Huang J, Wen ZQ, Xu N, Liu X, et al. miRNA expression profile in the N2 phenotype neutrophils of colorectal cancer and screen of putative key miRNAs. Cancer Manage Res. 2020;12:5491–503.
35. Tavora B, Mederer T, Wessel KJ, Ruffing S, Sadjadi M, Missmahl M, et al. Tumoural activation of TLR3-SLIT2 axis in endothelium drives metastasis. Nature. 2020;586(7828):299–304.
36. Xia Y, Wang L, Xu Z, Kong R, Wang F, Yin K, et al. Reduced USP33 expression in gastric cancer decreases inhibitory effects of Slit2-Robo1 signalling on cell migration and EMT. Cell Prolif. 2019;52(3):e12606.
37. Shi R, Yang Z, Liu W, Liu B, Xu Z, Zhang Z. Knockdown of Slit2 promotes growth and motility in gastric cancer cells via activation of AKT/β-catenin. Oncol Rep. 2014;31(2):812–8.
38. Li L, Zuo X, Liu D, Luo H, Zhu H. The profiles of miRNAs and lncRNAs in peripheral blood neutrophils exosomes of diffuse cutaneous systemic sclerosis. J Dermatol Sci. 2020;98(2):88–97.
39. Ye R, Lin Q, Xiao W, Mao L, Zhang P, Zhou L, et al. Mir-150-5p in neutrophil-derived extracellular vesicles associated with sepsis-induced cardiomyopathy in septic patients. Cell Death Discovery. 2023;9(1):19.

Publisher's note